

Band offsets in heterojunctions between cubic perovskite oxides

Alexander I. Lebedev*

*Physics Department, Moscow State University,
Leninskie gory, 119991 Moscow, Russia*

(Dated: February 28, 2024)

The band offsets for nine heterojunctions between titanates, zirconates, and niobates with the cubic perovskite structure were calculated from first principles. The effect of strain in contacting oxides on their energy structure, many-body corrections to the position of the band edges (calculated in the *GW* approximation), and the splitting of the conduction band resulting from spin-orbit interaction were consistently taken into account. It was shown that the neglect of the many-body effects can lead to errors in determination of the band offsets up to 0.36 eV. The failure of the transitivity rule, which is often used to determine the band offsets in heterojunctions, was demonstrated and its cause was explained.

PACS numbers: 68.65.Cd, 73.40.-c, 77.84.-s, 79.60.Jv

I. INTRODUCTION

Almost all electronic and optoelectronic devices contain metal–semiconductor, metal–dielectric, semiconductor–dielectric, or semiconductor–semiconductor interfaces. As the energy of an electron abruptly changes at the interface, the characteristics of devices that include such interfaces directly depend on the height of emerging energy barriers. Originally, the concept of a heterojunction was associated with a contact between two semiconductors, but currently its use is significantly expanded to include dielectrics. For example, in solving the actual problem of replacing the SiO₂ gate dielectric in silicon field-effect transistors with a material with higher dielectric constant, the calculation of the tunneling current through the gate dielectric requires an accurate knowledge of the energy diagram of the formed heterojunction.

In the last decade, experimental studies have discovered a number of new physical phenomena occurring at the interface of two oxide dielectrics. These include the appearance of a quasi-two-dimensional electron gas (2DEG) at the interface of two dielectrics¹ and its superconductivity;² the magnetism at the interface of two non-magnetic oxides.³ The ability to control the conductivity of the 2DEG with an electric field (an analog of the field effect)^{4,5} and so to control the temperature of the superconducting phase transition⁶ were demonstrated. The strongest conductivity changes were observed when one of the oxides was ferroelectric.⁷ When the components of heterostructures were magnetic and ferroelectric oxides, the ability to control the magnetic properties of the structure with a switchable ferroelectric polarization was shown.^{8–10} Thus, these heterostructures acquired the properties of a multiferroic. The above-mentioned and other interesting phenomena observed in oxide heterostructures open new opportunities for developing of new multifunctional electronic devices and suggest the emergence of a new direction in microelectronics, the oxide electronics.^{11–13}

The development of the ferroelectric memory devices

is one of the applications of the ferroelectric oxides. It requires to solve the problem of non-destructive read-out of information and to increase the packing density of the memory cells. For non-destructive optical read-out methods, the memory cell size is limited by the wave length. For titanates with the perovskite structure, in which the typical band gap is ~ 3 eV, the minimum cell size is ~ 4000 Å. In multiferroics, in which the information is stored electrically and read out magnetically, the memory cell size can be reduced to the size typical for modern hard disks, ~ 500 Å (in homogeneous multiferroic thin film, the physical size of the memory cells is limited by a rather large width of magnetic domain wall).

The methods based on the electrical read-out of the ferroelectric polarization are the most promising. Since the physical size of the ferroelectric memory cells is limited by the thickness of the ferroelectric domain wall and the minimum film thickness for which the ferroelectricity still exists (both sizes are a few unit cells^{14–17}), the packing density of the memory cells in these devices is maximized. These methods can be based, for example, on the nonlinear current-voltage characteristics which are reversible upon switching the polarization in the metal–ferroelectric–metal structures as demonstrated on thin films of PZT¹⁸ and BiFeO₃.^{19,20} A similar behavior can be observed on the structures that use the tunneling through a thin layer of ferroelectric.^{21–23}

The most important physical parameters that characterize an interface between two semiconductors or dielectrics are the band offsets on the energy diagram of the heterojunction. The valence band offset ΔE_v (the conduction band offset ΔE_c) is defined as the difference between the energies of the tops of the valence bands (bottoms of the conduction bands) in two contacting materials. These band offsets determine a number of physical properties of heterojunctions, in particular, their electrical and optical properties.

For oxides with the perovskite structure, the reliable experimental data on the band offsets (obtained by the photoelectron spectroscopy) exist for heterojunctions SrTiO₃/Si,^{24–26} BaTiO₃/Si,²⁶

SrTiO₃/GaAs,^{27,28} BaTiO₃/Ge,²⁹ SrTiO₃/InN,^{30,31} BaTiO₃/InN,³¹ SrTiO₃/ZnO,³¹ BaTiO₃/ZnO,^{31,32} SrTiO₃/SrO,³³ and BaTiO₃/BaO.³³ For heterojunctions between two perovskite dielectrics, the data are limited by the PbTiO₃/SrTiO₃,³⁴ SrTiO₃/SrZrO₃,³⁵ SrTiO₃/LaAlO₃,^{36,37} and SrTiO₃/BiFeO₃³⁸ systems. In addition, there are data on the Schottky barrier heights for perovskite-metal structures, in which the metals are Pt, Au, Ag, or the conductive oxides SrRuO₃ and (La,Sr)CoO₃.

In this work, the band offsets for nine heterojunctions between titanates, zirconates, and niobates with the cubic perovskite structure are calculated from first principles using the density functional theory and *GW* approximation. The obtained results are compared with available experimental data.

II. METHODOLOGY

The band offsets cannot be determined from a direct comparison of the energies of the valence and conduction bands obtained from the first-principles band-structure calculations performed separately for two constituent bulk materials. This is because in the first-principles calculations, there is no intrinsic energy scale: the energies corresponding to the valence band edge E_v and to the conduction band edge E_c are usually measured from an average of the electrostatic potential, which is an ill-defined quantity for infinite systems. Consequently, in addition to the band-structure calculations for two materials, the lineup of the average of the electrostatic potential ΔV between them should also be calculated. The latter value is determined by the dipole moment emerging at the heterojunction as a result of the redistribution of the electron density on the hybridized orbitals in the constituent materials. It takes into account all the features typical of the interface, such as the change in the chemical composition, the structure distortions, etc.

Thus, the valence band offset can be represented as a sum of two terms:³⁹

$$\Delta E_v = (E_{v2} - E_{v1}) + \Delta V. \quad (1)$$

The first term in this equation is the difference of the energies corresponding to the tops of the valence bands in two bulk materials. It can be obtained from standard band-structure calculations.

The second term in Eq. (1) is the lineup of the average of the electrostatic potential through the heterojunction. To calculate ΔV , one usually starts from the total potential (the potential of the ions plus the microscopic electrostatic Hartree potential for electrons) obtained from the self-consistent electron density calculation in a superlattice constructed of the contacting materials. After that, the macroscopic averaging technique⁴⁰ is applied, in which the electrostatic potential is first averaged over planes parallel to the interface and then the convolution of the obtained one-dimensional quasi-periodic function

with two rectangular windows whose lengths are determined by the periods of components is calculated. The resulting profiles of the macroscopic average of the electrostatic potential $\bar{V}(r)$ have flat (bulk-like) regions far enough from the interface. The ΔV value is defined as the difference energy between these plateau values. It should be noted that neither the E_{v1} and E_{v2} quantities, nor ΔV does not have physical meaning themselves, only the sum, Eq. (1), is meaningful.

The conduction band offset is calculated from the ΔE_v value and the difference of the band gaps in two materials:

$$\Delta E_c = (E_{c2} - E_{c1}) + \Delta V = (E_{g2} - E_{g1}) + \Delta E_v.$$

Roughly, the band gap $E_g = E_c - E_v$ can be estimated in the LDA approximation for the exchange-correlation energy. However, because of the well-known band-gap problem characteristic of this one-electron approximation, more accurate calculations should take into account the corrections to the band energies resulting from many-body effects. These corrections (the values ΔE_c^{QP} and ΔE_v^{QP}) are usually calculated in the quasiparticle *GW* approximation. It is usually believed that many-body corrections adjust the position of the conduction band and in this way solve the band-gap problem, however, the energy levels in the valence band are also corrected.

In the case of well-studied materials, the ΔE_c value is often calculated from the experimental band gaps. However, if the band offset ΔE_v was obtained theoretically, the problem associated with the uncertainty in the ΔE_v^{QP} values remains. It is often assumed that the ΔE_v^{QP} values in two materials are close, so that their contributions to the band offsets cancel each other. In this work, we show that this assumption in general is not true.

It should be also noted that, since the position of the energy levels in a crystal depends on the interatomic distances, the calculation of E_{v1} , E_{c1} , E_{v2} , and E_{c2} should be carried out under the same strain of materials, which appears in a heterojunction. Besides the strain-induced lifting of the degeneracy of the band edges, the band gap itself can vary. Moreover, the calculations should take into account the possible lifting of the band degeneracy resulting from spin-orbit interaction. Although the structure of dielectrics—the lattice parameters and equilibrium atomic positions—are weakly dependent on the spin-orbit interaction (and therefore it is usually neglected in the calculations), in the band structure calculations, the spin-orbit interaction strongly affects the energy position of the bands, and it cannot be neglected. In dielectrics, the taking into account of the spin-orbit interaction can be done *a posteriori*, after completion of the main first-principles calculations.

III. THE CALCULATION TECHNIQUE

The objects of the present calculations were heterojunctions formed between titanates and zirconates of

calcium, strontium, barium, and lead as well as the $\text{KNbO}_3/\text{NaNbO}_3$ heterojunction. They were modeled using superlattices grown in the $[001]$ direction and consisted of two materials with equal thickness of layers, each of four unit cells. The in-plane lattice parameter was obtained from the condition of zero stress at the interface (i.e., it was close to the lattice parameter of the solid solution with the component ratio of 1:1); the period of the superlattice and atomic displacements normal to the interface were fully relaxed.

The equilibrium lattice parameters and atomic positions were calculated from first principles within the density functional theory (DFT) using the **ABINIT** software. The exchange-correlation interaction was described in the local density approximation (LDA). Pseudopotentials of the atoms were taken from Refs. 41 and 42. The maximum energy of plane waves was 30 Ha (816 eV). For the integration over the Brillouin zone, the $8 \times 8 \times 2$ Monkhorst-Pack mesh was used. All calculations were performed for heterojunctions between cubic $Pm3m$ phases; the possible polar and antiferrodistortive (structural) distortions of the materials were neglected (they will be considered in a separate paper). The ΔV value was determined using the macroscopic averaging technique.⁴⁰ To determine the values of E_{v1} , E_{c1} , E_{v2} , and E_{c2} in constituent materials, similar calculations were performed for isolated crystals with the in-plane lattice parameter equal to that of the superlattice; in the normal direction the crystals were stress-free.

The calculations of the quasiparticle band gap and the many-body corrections to the position of the band edges were carried out in the so-called one-shot *GW* approximation.⁴³ The Kohn-Sham wave functions and energies calculated within the DFT-LDA approach were used as a zeroth-order approximation. The dielectric matrix $\epsilon_{\mathbf{G}\mathbf{G}'}(\mathbf{q}, \omega)$ was calculated for a $6 \times 6 \times 6$ mesh of wave vectors \mathbf{q} from the matrix of irreducible polarizability $P_{\mathbf{G}\mathbf{G}'}^0(\mathbf{q}, \omega)$ calculated for 2200–2800 vectors $\mathbf{G}(\mathbf{G}')$ in reciprocal space, 20–22 filled and 278–280 empty bands. Dynamic screening was described in the Godby–Needs plasmon-pole model. The wave functions with the energies up to 24 Ha were taken into account in the calculations. The energy corrections to the LDA solution were calculated from the diagonal matrix elements of $[\Sigma - E_{xc}]$ operator, where $\Sigma = GW$ is the self energy operator, E_{xc} is the operator of the exchange-correlation energy, G is the Green’s function, and $W = \epsilon^{-1}v$ is the screened Coulomb interaction. In calculating Σ , the wave function with the energies up to 24 Ha were taken into account.

IV. RESULTS

Fig. 1 shows the steps of the energy diagram calculation for a typical heterojunction. The extreme left and right parts in the figure correspond to the individual compounds with the cubic $Pm3m$ structure, whose lattice parameter corresponds to zero external stress. Bi-

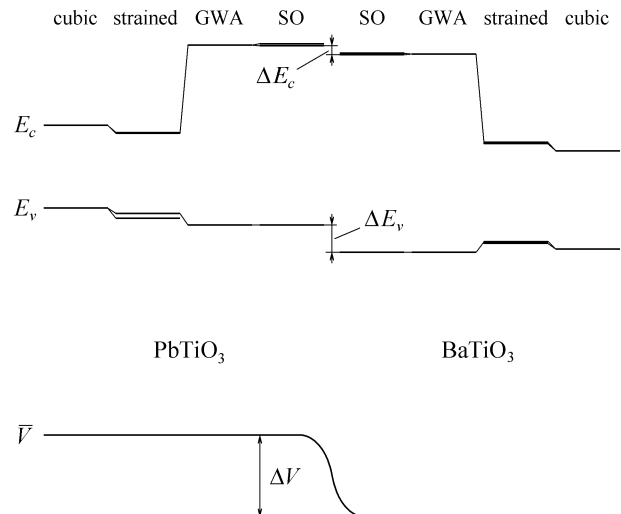


FIG. 1. The steps of the band offsets calculation for the $\text{PbTiO}_3/\text{BaTiO}_3$ heterojunction. First, the changes in the band structure of cubic phases induced by the strain in the heterojunction are taken into account, then the corrections resulting from the many-body effects are applied (GWA), and finally, the splitting of the band edges caused by the spin-orbit interaction (SO) is taken into account. The bottom chart shows the change of the average of the electrostatic potential in the heterojunction, which is a reference energy level for all bands.

axial strain of these compounds during the formation of the heterojunction (their in-plane lattice parameters become equal), reduces the symmetry of their unit cells to $P4/mmm$. As a result, their band gaps are changed and the degeneracy of the energy levels at some points of the Brillouin zone are lifted. For example, the three-fold degeneracy of the conduction band at the Γ point and that of the valence band at the R point are lifted (Fig. 2). These band extrema locations are typical for all compounds studied in this work except for PbTiO_3 and PbZrO_3 . In cubic PbTiO_3 , the top of the valence band is at the X point, and the tetragonal distortion removes the valley degeneracy (depending on the sign of the strain, the valence band edge is located at either X or Z point of the Brillouin zone of the tetragonal lattice). In cubic PbZrO_3 , the only compound in which both band extrema are located at the X point, the strain also removes the valley degeneracy, but both extrema remain at the same point of the Brillouin zone (X or Z). The energy diagrams of strained crystals are shown in Fig. 1 next to the diagrams for cubic phases. We note that not only the band gap, but also the energies of the band edges (E_c and E_v) measured from the averaged electrostatic potential are changed upon strain. The values of these energies in strained crystals are given in Tables I and II.

The calculation of the many-body corrections to the positions of the valence band edge ΔE_v^{QP} and of the conduction band edge ΔE_c^{QP} in the *GW* approximation

TABLE I. Parameters determining the valence band offset ΔE_v on the energy diagram of heterojunctions (all the energies are in eV).

Heterojunction	E_{v2}	$\Delta E_{v2}^{\text{QP}}$	E_{v1}	$\Delta E_{v1}^{\text{QP}}$	ΔV	ΔE_v
SrTiO ₃ /PbTiO ₃	13.629	-0.239	15.464	-0.315	+2.143	+0.384
BaTiO ₃ /BaZrO ₃	13.422	-0.512	13.766	-0.226	+0.066	-0.564
PbTiO ₃ /PbZrO ₃	12.390	-0.321	13.123	-0.239	+0.495	-0.320
PbTiO ₃ /BaTiO ₃	14.291	-0.226	13.453	-0.239	-1.276	-0.425
SrTiO ₃ /BaTiO ₃	14.366	-0.226	15.333	-0.315	+0.864	-0.014
SrTiO ₃ /SrZrO ₃	14.391	-0.582	14.912	-0.315	+0.395	-0.393
PbZrO ₃ /BaZrO ₃	13.158	-0.512	11.888	-0.321	-1.209	-0.130
SrTiO ₃ /CaTiO ₃	15.631	-0.333	15.664	-0.315	+0.131	+0.080
KNbO ₃ /NaNbO ₃	13.617	-0.314	14.494	-0.245	+0.944	-0.002

TABLE II. Parameters determining the conduction band offset ΔE_c on the energy diagram of heterojunctions and the type of the heterojunction (all the energies are in eV).

Heterojunction	E_{c2}	$\Delta E_{c2}^{\text{QP}}$	$\Delta E_{c2}^{\text{SO}}$	E_{c1}	$\Delta E_{c1}^{\text{QP}}$	$\Delta E_{c1}^{\text{SO}}$	ΔE_c	Type
SrTiO ₃ /PbTiO ₃	14.899	+1.326	-0.010	17.034	+1.431	-0.007	-0.100	I
BaTiO ₃ /BaZrO ₃	16.363	+1.199	-0.026	15.143	+1.341	-0.008	+1.126	I
PbTiO ₃ /PbZrO ₃	14.513	+0.266	0	14.269	+1.326	-0.010	-0.311	II
PbTiO ₃ /BaTiO ₃	15.820	+1.341	-0.008	14.704	+1.326	-0.010	-0.143	II
SrTiO ₃ /BaTiO ₃	15.885	+1.341	-0.008	16.879	+1.431	-0.007	-0.221	II
SrTiO ₃ /SrZrO ₃	17.469	+1.283	-0.023	16.347	+1.431	-0.007	+1.353	I
PbZrO ₃ /BaZrO ₃	16.116	+1.199	-0.026	14.069	+0.266	0	+1.745	I
SrTiO ₃ /CaTiO ₃	17.207	+1.486	-0.007	17.237	+1.431	-0.007	+0.156	II
KNbO ₃ /NaNbO ₃	15.005	+1.008	-0.038	15.823	+0.976	-0.037	+0.157	I

shows that the many-body effects shift the position of the conduction band up by ~ 1.3 eV in all compounds studied in this work except for PbZrO₃ in which the shift is only 0.266 eV (Tables I and II). The valence band edge is shifted down by 0.22–0.58 eV on taking into account the many-body effects. Although the absolute values of these corrections slowly converge with increasing number of empty bands in the *GW* calculations (see, for example, Ref. 44), the relative shift of the difference between the corrections in different compounds is small. Therefore, if one uses the same total number of bands (300 in our case) in the calculations of these corrections, the error in determination of the relative position of the band edges in two materials is not large, ~ 0.01 eV according to our estimates. In our calculations we have also assumed that the many-body corrections slightly depend on the strain, and so the values calculated for the cubic crystals can be used. The tests have shown that the strain-induced changes of ΔE_v^{QP} and ΔE_c^{QP} may reach 0.01–0.02 eV, which gives an estimate of possible errors. The energy diagrams of constituent materials after accounting for many-body effects are also shown in Fig. 1.

The calculations of many-body corrections show that the assumption used by many authors about an approximate equality of these corrections in two contacting materials, in general, is not true. It is seen that in related

oxides with the cubic perovskite structure the scatter of the ΔE_v^{QP} values can be as large as 0.36 eV. This value is a measure of the possible error in determination of the band offsets in the calculations that neglect the many-body effects.⁴⁵

Since our crystals contain atoms with a large atomic number, the errors in determination of the band edge positions resulting from the neglect of the spin-orbit interaction can be quite large. In this work, the spin-orbit splitting Δ_{SO} of the valence and conduction band edges was calculated using the full-relativistic pseudopotentials.⁴⁶ The tests performed on a number of semiconductors (Ge, GaAs, CdTe), for which the spin-orbit splitting of the valence band is accurately measured, showed that the Δ_{SO} values calculated in this way agree with experiment to within $\sim 5\%$.

The calculations showed that the spin-orbit interaction results in a splitting of the band edges at some points of the Brillouin zone. First of all, it refers to the conduction band edge at the Γ point. It is interesting that despite the presence of heavy atoms such as Ba and Pb in our crystals, the spin-orbit splitting is not very large. This is because the conduction band states at the Γ point in these crystals are formed primarily from the *d*-states of the *B* atom (Ti, Zr, Nb). The values Δ_{SO} of the spin-orbit splitting of the conduction band at the Γ point for

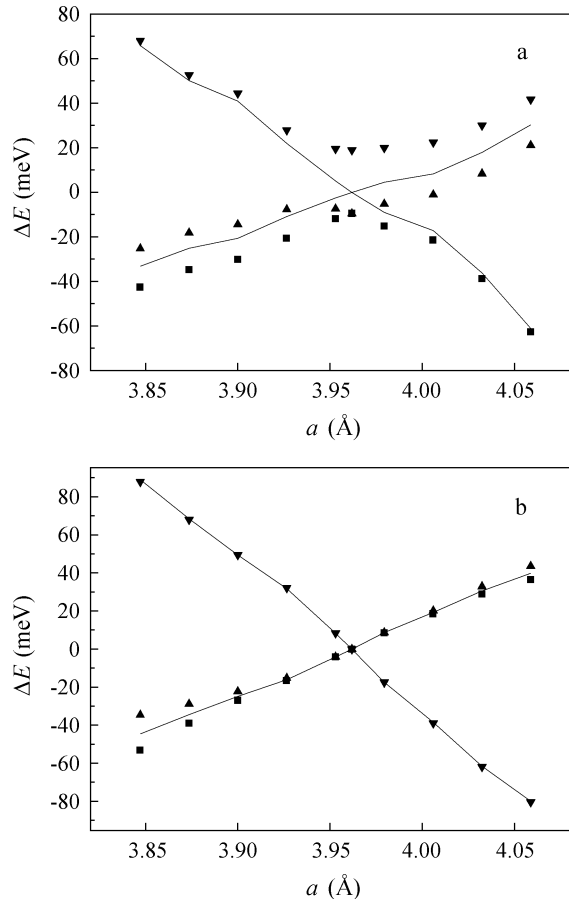


FIG. 2. Effect of biaxial strain on the splitting of the conduction band (a) and of the valence band (b) in BaTiO₃ without the spin-orbit interaction (lines) and with it (dots). The lattice parameter of stress-free (cubic) crystal is 3.962 Å.

all materials studied except for PbZrO₃ are given in Table III. In PbZrO₃, the conduction band minimum is located at the *X* point, is non-degenerate, and does not exhibit the spin-orbit splitting. The valence band edge (at *R* and *X* points) in all cubic crystals studied in this work does not exhibit the spin-orbit splitting too.

When the spin-orbit interaction is turned on, the center of gravity of the split energy levels coincides with the position of the energy level without spin-orbit interaction.⁴⁷ In all studied crystals, the spin-orbit split-off conduction band at the Γ point is always shifted to higher energies, and so the absolute minimum of the conduction band at the Γ point is shifted down by $\Delta_{SO}/3$. This value is given in Table II and determines an additional shift of the conduction band. The final energy diagram of the heterojunction obtained after taking into account the spin-orbit interaction is shown by two internal diagrams in Fig. 1. We note that in these calculations, we have neglected the weaker effects associated with the change of the band splitting; they result from the strain-induced

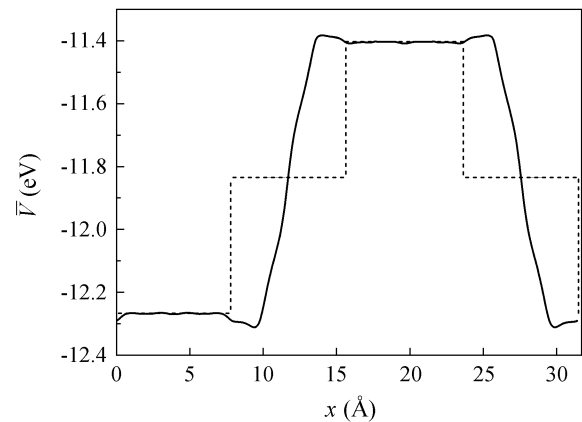


FIG. 3. Determination of the ΔV from the profile of the average electrostatic potential $\bar{V}(x)$ for the SrTiO₃/BaTiO₃ superlattice (solid line). The dotted line shows the approximating function.

mixing of different states and can be seen in Fig. 2. These effects, however, do not exceed 10 meV and are less than other systematic errors in our calculations.

In calculating the ΔV value, the profile of the electrostatic potential $\bar{V}(x)$ obtained with the macroscopic averaging technique was approximated by a step function with a width of transition regions of one lattice parameter (Fig. 3). The tests showed that when the thickness of the individual layers in the BaTiO₃/SrTiO₃ superlattice was changed from three to five unit cells, the variation in the ΔV value computed by the above algorithm was only ~ 4 meV, which gives an estimate of the error in the ΔV calculation. As shown in Ref. 48, the many-body effects do not influence much on the ΔV value.

The results of the band offsets calculations for nine heterojunctions are given in Tables I and II. The signs of the band offsets are defined as the energy change when moving from the compound indicated the first in the heterojunction pair to the compound indicated the second. The energy diagrams of heterojunctions are classified as type I heterojunctions, for which ΔE_c and ΔE_v have opposite signs, and type II heterojunctions, for which the signs of ΔE_c and ΔE_v are the same. The types of the heterojunctions are given in Table II and their energy diagrams are shown in Fig. 4.

V. DISCUSSION

Unfortunately, the experimental data on the band offsets in heterojunctions between oxides with the perovskite structure are very limited. In Ref. 35, the band offsets for the SrTiO₃/SrZrO₃ heterojunction were obtained using the photoelectron spectroscopy. According to these measurements, the heterojunction is type I, and the band offsets are $\Delta E_v = -0.5 \pm 0.15$ eV and

TABLE III. The spin-orbit splitting Δ_{SO} of the conduction band at the Γ point in cubic perovskites (in meV).

CaTiO ₃	SrTiO ₃	BaTiO ₃	PbTiO ₃	SrZrO ₃	BaZrO ₃	NaNbO ₃	KNbO ₃
20.7	22.0	25.3	28.5	70.2	77.5	113.7	111.0

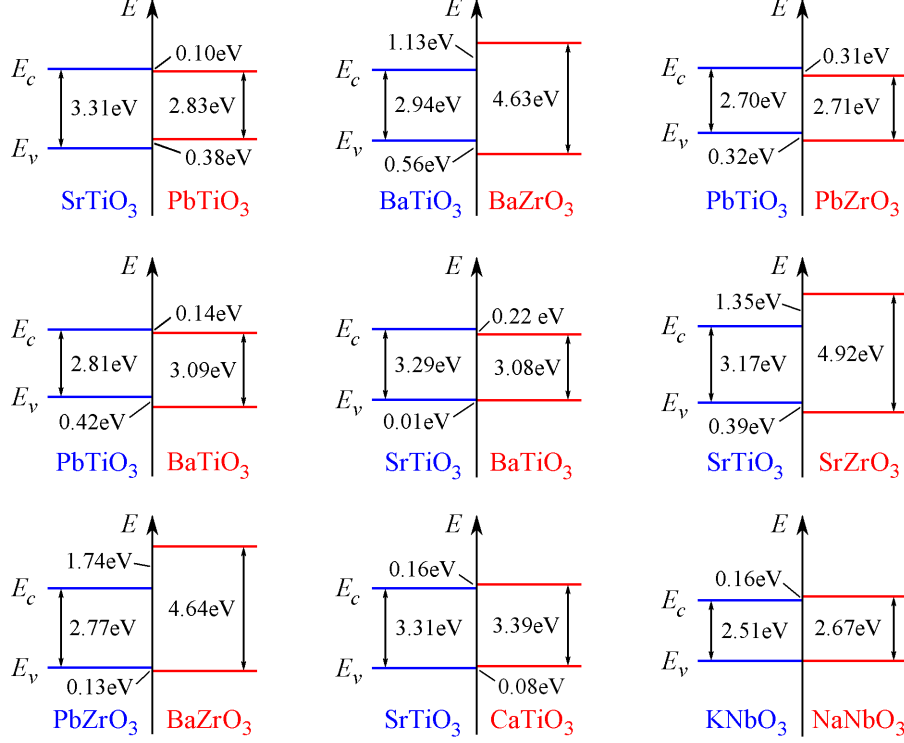


FIG. 4. (Color online) Energy diagrams for heterojunctions between cubic perovskites studied in this work.

$\Delta E_c = +1.9 \pm 0.15$ eV (in SrTiO₃ the valence band lies higher than in SrZrO₃). Our data agree well with these experimental data: according to our calculations, the heterojunction is also type I, and the band offsets are -0.393 and $+1.353$ eV, respectively, for *cubic* components.⁴⁹ We note that the band offsets predicted in this work are in much closer agreement with experiment compared to the results of Ref. 50 ($\Delta E_v = +0.5$ eV, $\Delta E_c = +2.5$ eV).

As the experimental SrTiO₃/SrZrO₃ structure³⁵ was grown on SrTiO₃ substrate, the calculated band offsets, which depend on the in-plane lattice parameter, may be slightly different (this dependence is well known for semiconductor heterojunctions^{39,47,51}). To estimate these changes, the calculations for the SrTiO₃/SrZrO₃ heterojunction were repeated for the in-plane lattice parameter equal to that of SrTiO₃. They gave $\Delta E_v = -0.240$ eV and $\Delta E_c = +1.230$ eV, which somewhat worsened the agreement with experiment.

It should be stressed that the results obtained in this work are for heterojunctions formed between *cubic* compounds. We deliberately did not take into account possible distortions of the perovskite structure, which obvi-

ously affect the energy diagram of heterojunctions. This is because the question about the character of these distortions is not so simple. It is known that the character of distortions in the perovskites may change significantly under the biaxial strain and, moreover, the distortions in two materials usually are highly interconnected. These effects are well known for ferroelectric superlattices.^{42,52–54} In heterojunctions between polar materials, the need to meet the electrical boundary conditions (equal electric displacement fields normal to the interface) causes the polarization in both constituent materials to differ from their equilibrium values. Since the accompanying atomic displacements affect the band gap and the positions of the band edges, in polar heterojunctions the band offsets can be very different from those in nonpolar structures.⁵⁵ In addition, the cases are known when the periodic domain structure can occur in a ferroelectric near the interface.⁵⁶ Predicting of the energy diagram for such a system is particularly problematic.

The experimental data for the SrTiO₃/PbTiO₃ heterojunction³⁴ are noticeably different from the results of our calculations. According to the photoelectron spectroscopy data, this heterojunction is type II and the

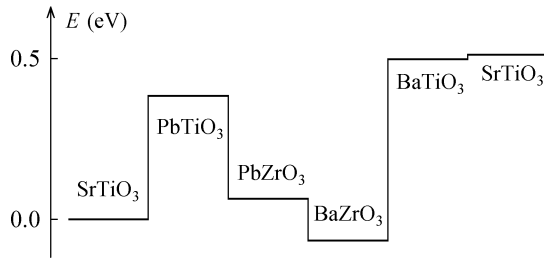


FIG. 5. Changes of the valence band position when traversing the contour $\text{SrTiO}_3/\text{PbTiO}_3/\text{PbZrO}_3/\text{BaZrO}_3/\text{BaTiO}_3/\text{SrTiO}_3$.

band offsets are $\Delta E_v = +1.1 \pm 0.1$ eV and $\Delta E_c = +1.3 \pm 0.1$ eV (in PbTiO_3 the valence band lies higher than in SrTiO_3). According to our calculations, the band offsets are $+0.384$ and -0.100 eV, respectively, and the heterojunction is type I. We see that in experiment and calculations, the signs of ΔE_v are the same, but their values differ considerably. The fact that the crystal structure of PbTiO_3 at 300 K is tetragonal cannot explain such a large discrepancy. A possible explanation is given below.

If the interface is not perfect (for example, in the case when the structural relaxation of strained materials occurs, as one can see in Refs. 35 and 38), the dangling bonds are created near the interface and the surface states appear in the electronic structure. These states are electrically active and can significantly disturb the ΔV value, and so to change ΔE_c and ΔE_v . In addition, in the relaxation region where the lattice parameter depends on the coordinate, an additional drift of the E_v and E_c values (the band bending) occurs. The distortion of the energy diagrams similar to that arising from the surface states can occur in heterojunctions between highly defective materials. Like the levels of the surface states, defects in constituent materials can exchange electrons with each other, which would distort the energy diagram of a heterojunction. The size of the region in which such an exchange occurs is about the screening length in a material and can be quite small. For example, in a dielectric with a defect concentration of 10^{18} cm^{-3} , the length of the impurity screening can be as small as 43 \AA .⁵⁷ It is possible that the strong discrepancy between the calculated and experimental band offsets in the $\text{SrTiO}_3/\text{PbTiO}_3$ heterojunction results from the presence of defects in materials: the band offsets observed in this heterojunction correspond to the case where the defect levels in two contacting materials are close in energy.³⁴ Even stronger distortions of the band diagram can be characteristic of heterostructures between perovskites with so-called valence discontinuity, such as $\text{SrTiO}_3/\text{LaAlO}_3$ (Ref. 36 and 37) and $\text{BiFeO}_3/\text{SrTiO}_3$ (Ref. 38), in which the distribution of the quasi-two-dimensional electron gas density is

different from that of the positive (ionic) charge.

In conclusion, we discuss the applicability of the transitivity rule which is often used to calculate the band offsets in heterojunctions by comparing the band offsets in a pair of heterojunctions formed between the components of the heterojunction under discussion and the third common component (see, for example, Refs. 34 and 58). From the heterojunctions we have studied, three closed chains (contours) can be formed in which the initial and the terminal components are the same: $\text{SrTiO}_3/\text{PbTiO}_3/\text{BaTiO}_3/\text{SrTiO}_3$, $\text{BaTiO}_3/\text{PbTiO}_3/\text{PbZrO}_3/\text{BaZrO}_3/\text{BaTiO}_3$, and $\text{SrTiO}_3/\text{PbTiO}_3/\text{PbZrO}_3/\text{BaZrO}_3/\text{BaTiO}_3/\text{SrTiO}_3$. The positions of the valence bands calculated from the obtained ΔE_v values for one of these chains is shown in Fig. 5. When traversing the contour, we never get zero (see the figure), the deviation is from -0.027 to $+0.539$ eV. This means that the transitivity rule is not applicable. The reason for this behavior is that in heterojunctions, the band offsets actually depend on the in-plane lattice parameter.^{33,39,47,51} If the lattice parameter in all the members of the chain would be the same, then traversing the contour would result in zero E_v shift.⁵⁹ However, because all heterojunctions in the above chains have different lattice parameters, the result is nonzero. Thus, in general, the transitivity rule is untenable, and the corresponding error can exceed 0.5 eV.

VI. CONCLUSION

In this work, the band offsets for eight heterojunctions between titanates and zirconates of calcium, strontium, barium, and lead as well as for the $\text{KNbO}_3/\text{NaNbO}_3$ heterojunction with the cubic perovskite structure were calculated from first principles. The effect of strain in contacting oxides on their energy structure, many-body corrections to the position of the band edges (calculated in the *GW* approximation), and the splitting of the conduction band resulting from spin-orbit interaction were consistently taken into account. It was shown that the neglect of the many-body effects can lead to errors in determination of the band offsets up to 0.36 eV. The failure of the transitivity rule, which is often used to determine the band offsets in heterojunctions, was demonstrated and its cause was explained.

ACKNOWLEDGMENTS

This work was partially supported by the Russian Foundation for Basic Research grant No. 13-02-00724. The calculations were performed on the laboratory computer cluster and the “Chebyshev” supercomputer at Moscow State University.

-
- * swan@scon155.phys.msu.ru
- ¹ A. Ohtomo and H. Y. Hwang, *Nature* **427**, 423 (2004).
 - ² N. Reyren, S. Thiel, A. D. Caviglia, L. F. Kourkoutis, G. Hammerl, C. Richter, C. W. Schneider, T. Kopp, A.-S. Rüetschi, D. Jaccard, M. Gabay, D. A. Muller, J.-M. Triscone, and J. Mannhart, *Science* **317**, 1196 (2007).
 - ³ A. Brinkman, M. Huijben, M. van Zalk, J. Huijben, U. Zeitler, J. C. Maan, W. G. van der Wiel, G. Rijnders, D. H. A. Blank, and H. Hilgenkamp, *Nature Mater.* **6**, 493 (2007).
 - ⁴ S. Thiel, G. Hammerl, A. Schmehl, C. W. Schneider, and J. Mannhart, *Science* **313**, 1942 (2006).
 - ⁵ C. Cen, S. Thiel, G. Hammerl, C. W. Schneider, K. E. Andersen, C. S. Hellberg, J. Mannhart, and J. Levy, *Nature Mater.* **7**, 298 (2008).
 - ⁶ A. D. Caviglia, S. Gariglio, N. Reyren, D. Jaccard, T. Schneider, M. Gabay, S. Thiel, G. Hammerl, J. Mannhart, and J.-M. Triscone, *Nature* **456**, 624 (2008).
 - ⁷ C. H. Ahn, S. Gariglio, P. Paruch, T. Tybell, L. Antognazza, and J.-M. Triscone, *Science* **284**, 1152 (1999).
 - ⁸ X. Hong, A. Posadas, A. Lin, and C. H. Ahn, *Phys. Rev. B* **68**, 134415 (2003).
 - ⁹ T. Kanki, H. Tanaka, and T. Kawai, *Appl. Phys. Lett.* **89**, 242506 (2006).
 - ¹⁰ H. J. A. Molegraaf, J. Hoffman, C. A. F. Vaz, S. Gariglio, D. van der Marel, C. H. Ahn, and J.-M. Triscone, *Adv. Mater.* **21**, 3470 (2009).
 - ¹¹ J. Mannhart and D. G. Schlom, *Science* **327**, 1607 (2010).
 - ¹² P. Zubko, S. Gariglio, M. Gabay, P. Ghosez, and J.-M. Triscone, *Annu. Rev. Condens. Matter Phys.* **2**, 141 (2011).
 - ¹³ H. Y. Hwang, Y. Iwasa, M. Kawasaki, B. Keimer, N. Nagao, and Y. Tokura, *Nature Mater.* **11**, 103 (2012).
 - ¹⁴ J. Padilla, W. Zhong, and D. Vanderbilt, *Phys. Rev. B* **53**, R5969 (1996).
 - ¹⁵ B. Meyer and D. Vanderbilt, *Phys. Rev. B* **65**, 104111 (2002).
 - ¹⁶ J. Junquera and P. Ghosez, *Nature* **422**, 506 (2003).
 - ¹⁷ N. Sai, A. M. Kolpak, and A. M. Rappe, *Phys. Rev. B* **72**, 020101 (2005).
 - ¹⁸ J. Rodríguez Contreras, H. Kohlstedt, U. Poppe, R. Waser, C. Buchal, and N. A. Pertsev, *Appl. Phys. Lett.* **83**, 4595 (2003).
 - ¹⁹ T. Choi, S. Lee, Y. J. Choi, V. Kiryukhin, and S.-W. Cheong, *Science* **324**, 63 (2009).
 - ²⁰ C. Wang, K. Juan Jin, Z. Tang Xu, L. Wang, C. Ge, H. Bin Lu, H. Zhong Guo, M. He, and G. Zhen Yang, *Appl. Phys. Lett.* **98**, 192901 (2011).
 - ²¹ M. Y. Zhuravlev, R. F. Sabirianov, S. S. Jaswal, and E. Y. Tsybal, *Phys. Rev. Lett.* **94**, 246802 (2005).
 - ²² H. Kohlstedt, N. A. Pertsev, J. Rodríguez Contreras, and R. Waser, *Phys. Rev. B* **72**, 125341 (2005).
 - ²³ V. Garcia, S. Fusil, K. Bouzehouane, S. Enouz-Vedrenne, N. D. Mathur, A. Barthélémy, and M. Bibes, *Nature* **460**, 81 (2009).
 - ²⁴ S. A. Chambers, Y. Liang, Z. Yu, R. Droopad, J. Ramdani, and K. Eisenbeiser, *Appl. Phys. Lett.* **77**, 1662 (2000).
 - ²⁵ S. A. Chambers, Y. Liang, Z. Yu, R. Droopad, and J. Ramdani, *J. Vac. Sci. Technol. A* **19**, 934 (2001).
 - ²⁶ F. Amy, A. S. Wan, A. Kahn, F. J. Walker, and R. A. McKee, *J. Appl. Phys.* **96**, 1635 (2004).
 - ²⁷ Y. Liang, J. Curless, and D. McCready, *Appl. Phys. Lett.* **86**, 082905 (2005).
 - ²⁸ Z. Yang, W. Huang, and J. Hao, *Appl. Phys. Lett.* **103**, 031919 (2013).
 - ²⁹ M. K. Hudait, Y. Zhu, N. Jain, D. Maurya, Y. Zhou, and S. Priya, *J. Appl. Phys.* **114**, 024303 (2013).
 - ³⁰ Z. Li, B. Zhang, J. Wang, J. Liu, X. Liu, S. Yang, Q. Zhu, and Z. Wang, *Nanoscale Res. Lett.* **6**, 193 (2011).
 - ³¹ C. Jia, Y. Chen, X. Liu, S. Yang, and Z. Wang, in *Ferroelectrics—Characterization and Modeling*, edited by M. Lallart (InTech, 2011) Chap. 16, pp. 305–324.
 - ³² C. Jia, Y. Chen, X. Zhou, A. Yang, G. Zheng, X. Liu, S. Yang, and Z. Wang, *Appl. Phys. A* **99**, 511 (2010).
 - ³³ J. Junquera, M. Zimmer, P. Ordejón, and P. Ghosez, *Phys. Rev. B* **67**, 155327 (2003).
 - ³⁴ R. Schafraneck, S. Li, F. Chen, W. Wu, and A. Klein, *Phys. Rev. B* **84**, 045317 (2011).
 - ³⁵ R. Schafraneck, J. D. Baniecki, M. Ishii, Y. Kotaka, K. Yamanka, and K. Kurihara, *J. Phys. D: Appl. Phys.* **45**, 055303 (2012).
 - ³⁶ L. Qiao, T. C. Droubay, V. Shutthanandan, Z. Zhu, P. V. Sushko, and S. A. Chambers, *J. Phys.: Condens. Matter* **22**, 312201 (2010).
 - ³⁷ G. Berner, A. Müller, F. Pfaff, J. Walde, C. Richter, J. Mannhart, S. Thiess, A. Gloskovskii, W. Drube, M. Sing, and R. Claessen, *Phys. Rev. B* **88**, 115111 (2013).
 - ³⁸ R. Schafraneck, J. D. Baniecki, M. Ishii, Y. Kotaka, and K. Kurihara, *New J. Phys.* **15**, 053014 (2013).
 - ³⁹ L. Colombo, R. Resta, and S. Baroni, *Phys. Rev. B* **44**, 5572 (1991).
 - ⁴⁰ A. Baldereschi, S. Baroni, and R. Resta, *Phys. Rev. Lett.* **61**, 734 (1988).
 - ⁴¹ A. I. Lebedev, *Phys. Solid State* **51**, 362 (2009).
 - ⁴² A. I. Lebedev, *Phys. Solid State* **52**, 1448 (2010).
 - ⁴³ G. Onida, L. Reining, and A. Rubio, *Rev. Mod. Phys.* **74**, 601 (2002).
 - ⁴⁴ F. Bruneval and X. Gonze, *Phys. Rev. B* **78**, 085125 (2008).
 - ⁴⁵ A more detailed study have shown that in a large class of oxides, fluorides, and nitrides the variation in the $\Delta E_{\text{QP}}^{\text{QP}}$ values can reach 3 eV. These results and their explanation will be published in a separate paper.
 - ⁴⁶ C. Hartwigsen, S. Goedecker, and J. Hutter, *Phys. Rev. B* **58**, 3641 (1998).
 - ⁴⁷ C. G. Van de Walle and R. M. Martin, *Phys. Rev. B* **34**, 5621 (1986).
 - ⁴⁸ R. Shaltaf, G.-M. Rignanese, X. Gonze, F. Giustino, and A. Pasquarello, *Phys. Rev. Lett.* **100**, 186401 (2008).
 - ⁴⁹ If we take into account that the real structure of SrZrO_3 at 300 K is orthorhombic and the corresponding increase of the LDA band gap in this structure is 0.361 eV, the conduction band offset can be estimated as +1.714 eV. In this estimate, we neglected the changes of the many-body corrections upon structural distortion and supposed that the band gap correction changes only the location of the conduction band.
 - ⁵⁰ P. Delugas, A. Filippetti, A. Gadaleta, I. Pallecchi, D. Marré, and V. Fiorentini, *Phys. Rev. B* **88**, 115304 (2013).

- ⁵¹ D. Cociorva, W. G. Aulbur, and J. W. Wilkins, Solid State Commun. **124**, 63 (2002).
- ⁵² K. Johnston, X. Huang, J. B. Neaton, and K. M. Rabe, Phys. Rev. B **71**, 100103 (2005).
- ⁵³ L. Kim, J. Kim, U. V. Waghmare, D. Jung, and J. Lee, Phys. Rev. B **72**, 214121 (2005).
- ⁵⁴ A. I. Lebedev, Phys. Solid State **51**, 2324 (2009).
- ⁵⁵ The same reasoning applies to heterojunctions between semiconductors with the wurtzite structure like GaN/AlN in which both materials have nonzero spontaneous polarization.
- ⁵⁶ E. Bousquet, J. Junquera, and P. Ghosez, Phys. Rev. B **82**, 045426 (2010).
- ⁵⁷ L. M. Falicov and M. Cuevas, Phys. Rev. **164**, 1025 (1967).
- ⁵⁸ H. Kroemer, in *Molecular Beam Epitaxy and Heterostructures*, edited by L. L. Chang and K. Ploog (Springer Netherlands, 1985) pp. 331–379.
- ⁵⁹ This was indeed observed for three almost lattice-matched heterojunction pairs, Ge/GaAs, Ge/ZnSe, and GaAs/ZnSe.⁵⁸